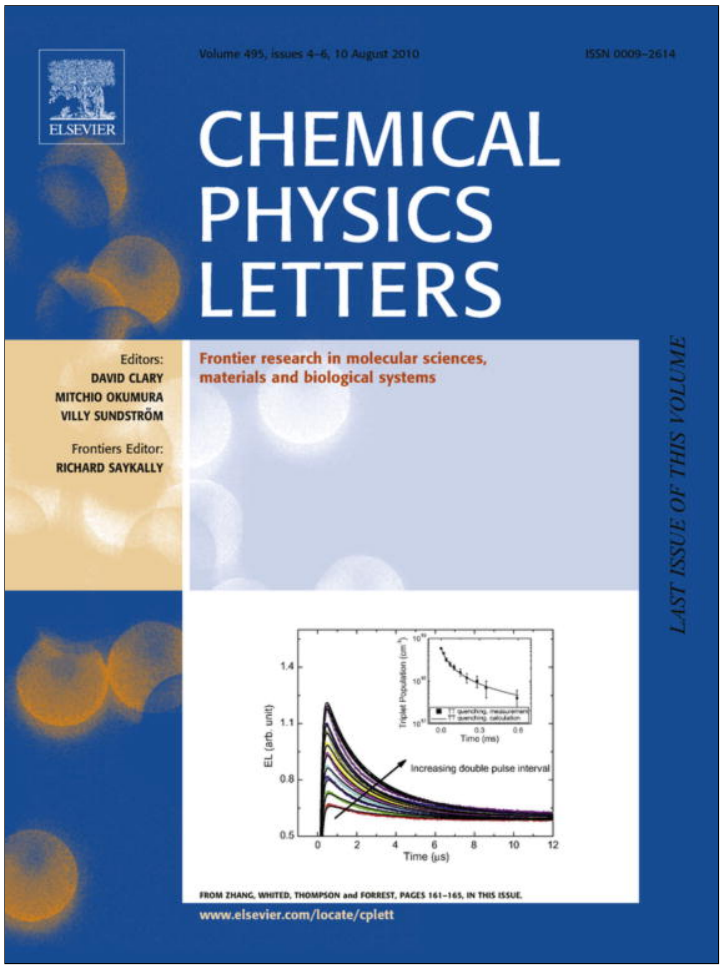

Chemical Physics Letters 495 (2010) 275–279

Contents lists available at ScienceDirect

Chemical Physics Letters

journal homepage: www.elsevier.com/locate/cplett

New fluorescent probes for detection and characterization of amyloid fibrils

Galyna Gorbenko [a,*], Valeriya Trusova [a], Elena Kirilova [b], Georgiy Kirilov [b], Inta Kalnina [b], Aleksey Vasilev [c], Stefka Kaloyanova [c], Todor Deligeorgiev [c]

[a] Department of Biological and Medical Physics, V.N. Karazin Kharkov National University, 4 Svobody Sq., Kharkov 61077, Ukraine
[b] Department of Chemistry and Geography, Faculty of Natural Sciences and Mathematics, Daugavpils University, 13 Vienibas, Daugavpils LV5401, Latvia
[c] Department of Applied Organic Chemistry, Faculty of Chemistry, University of Sofia, 1164 Sofia, Bulgaria

ARTICLE INFO

Article history:
Received 15 April 2010
In final form 1 July 2010
Available online 8 July 2010

ABSTRACT

The applicability of the novel fluorescent probes, aminoderivative of benzanthrone ABM, squaraine dye SQ-1 and polymethine dye V2 to identification and structural analysis of amyloid fibrils has been evaluated using the lysozyme model system in which fibrillar aggregates have been formed in concentrated ethanol solution. The association constant, binding stoichiometry and molar fluorescence of the bound dye have been determined. ABM was found to surpass classical amyloid marker ThT in the sensitivity to the presence of fibrillar aggregates. Resonance energy transfer measurements involving ABM–SQ-1 and SQ-1–V2 donor–acceptor pairs yielded the limits for fractal-like dimension of lysozyme fibrils.

1. Introduction

Due to intrinsic propensity of polypeptide chain for self-association, protein molecules are highly prone to forming different types of aggregates, from amorphous structures to crystals and amyloid fibrils [1]. The last type of protein aggregates, amyloid fibrils, currently is in a focus of the most extensive research efforts because their formation has been correlated with a number of so-called protein misfolding diseases, *viz.* neurological disorders, type II diabetes, spongiform encephalopathies, systemic amyloidosis, *etc.* [2,3]. These are highly ordered aggregates with a core cross-β-sheet structure, in which β-strands run perpendicularly to the long axis of the fibril, while β-sheets propagate in its direction [4]. Mature fibrils have a diameter 4–13 nm and usually contain from 2 to 6 laterally associated or twisted protofilaments, each 2–5 nm in diameter [5]. Experimental techniques currently used to detect fibrillar aggregates, include electron microscopy, FTIR, fluorescence and absorption spectroscopy [6,7]. One common criterion for identification of amyloid fibrils both *in vivo* and *in vitro* is based on the property of benzothiazole fluorescent dye thioflavin T (ThT) to interact specifically with fibrillar structures [8,9], producing markedly enhanced fluorescence and shift of emission maximum from 440 to 480 nm [10]. However, despite being widespread, ThT assay is not devoid of shortcomings associated, particularly, with (i) dependence of ThT spectral characteristics on fibril morphology [11], pH [12], ionic strength [13]; (ii) ThT ability to affect fibrillization kinetics and stability of fibrillar intermediates [14]; (iii) sensitivity of ThT fluorescence to the presence of exogenous compounds, for instance, polyphenols [15]. For this reason, a variety of new fluorophores is continuously testing for their amyloid specificity. These include Thioflavin S [16], K114 [17], X-34 [18], T-284 [19], PTAA [20], a series of cyanine dyes [21], luminescent conjugated polymers [22].

The present study has been undertaken to evaluate the possibility of using the novel fluorescent dye ABM, aminoderivative of benzanthrone, for identification of amyloid fibrils and uncovering their structural peculiarities. Previously it has been demonstrated that ABM possesses marked affinity for artificial lipid bilayers and cellular (lymphocyte) membranes, the property which renders this probe highly sensitive to the changes in immune status of a human organism at different pathologies [23–25]. However, ABM potential in characterization of conformationally-altered, oligomeric and fibrillar protein states has not yet been properly explored. In an attempt to fill this gap, our goal was threefold: (i) to examine ABM spectral behavior in the presence of native and fibrillar lysozyme; (ii) to compare ABM amyloid specificity with that of Thioflavin T; (iii) to assess what kind of information can be extracted from analyzing resonance energy transfer between fluorescent dyes associated with protein fibrils.

2. Materials and methods

2.1. Chemicals

Chicken egg white lysozyme was purchased from Sigma (St. Louis, MO, USA). ABM (3-morpholino-7H-benzo[de]anthracene-7-one) was synthesized at the Faculty of Natural Sciences and Mathematics of Daugavpils University by a nucleophilic substitution of the bromine atom in 3-bromobenzanthrone, as described

* Corresponding author. Address: 52-52 Tobolskaya Str., Kharkov 61072, Ukraine.
E-mail address: galyagor@yahoo.com (G. Gorbenko).

0009-2614/$ - see front matter © 2010 Elsevier B.V. All rights reserved.
doi:10.1016/j.cplett.2010.07.005

in more detail previously [26]. Squaraine dye SQ-1 and its structural analog, the polymethine dye V2, having the same end groups as SQ-1, but lacking the central squaric moiety, were synthesized at the Faculty of Chemistry, University of Sofia [27].

2.2. Preparation of lysozyme fibrils

The reaction of lysozyme fibrillization was initiated using the approach developed by Holley and coworkers [28]. Protein solutions (3 mg/ml) were prepared by dissolving lysozyme in deionized water with subsequent slow addition of ethanol to a final concentration 80%. Next, the samples were subjected to constant agitation at ambient temperature. This resulted in the formation of lysozyme fibrils over a time course of about 30 days. The amyloid nature of fibrillar aggregates was confirmed in ThT assay.

2.3. Fluorescence measurements

Steady-state fluorescence spectra were recorded with LS-55 spectrofluorometer equipped with a magnetically stirred, thermostated cuvette holder (Perkin–Elmer Ltd., Beaconsfield, UK). Fluorescence measurements were performed at 20 °C using 10 mm path-length quartz cuvettes. Emission spectra were recorded in buffer and in the presence of native or fibrillar lysozyme with excitation wavelengths of 430 nm (ABM), 440 nm (ThT) or 640 nm (SQ-1). Excitation and emission band passes were set at 10 nm.

Quantitative parameters of the dye–protein interactions (association constant (K_a), binding stoichiometry (n) and molar fluorescence of the bound dye (a) have been determined by describing the lysozyme-induced changes of the dye fluorescence ($\Delta I(C_P)$) in terms of the Langmuir adsorption model:

$$\Delta I = 0.5a\left[Z_o + nC_P + 1/K_a - \sqrt{(Z_o + nC_P + 1/K_a)^2 - 4nC_PZ_o}\right] \quad (1)$$

where Z_o, C_P are the total concentrations of the dye and protein, respectively. The dye concentrations were determined spectrophotometrically, using extinction coefficients $\varepsilon_{444} = 2.1 \times 10^4\ M^{-1}\ cm^{-1}$ (ABM), $\varepsilon_{662} = 2.3 \times 10^5\ M^{-1}\ cm^{-1}$ (SQ-1), $\varepsilon_{685} = 2.5 \times 10^5\ M^{-1}\ cm^{-1}$ (V2) and $\varepsilon_{412} = 3.6 \times 10^4\ M^{-1}\ cm^{-1}$ (ThT).

The critical distance of energy transfer was calculated as [29]:

$$R_o = 979(\kappa^2 n_r^{-4} Q_D J)^{1/6},$$
$$J = \int_0^\infty F_D(\lambda)\varepsilon_A(\lambda)\lambda^4 d\lambda \Big/ \int_0^\infty F_D(\lambda)d\lambda \quad (2)$$

where J is the overlap integral derived from numerical integration, $F_D(\lambda)$ is the donor fluorescence intensity, $\varepsilon_A(\lambda)$ is the acceptor molar absorbance at the wavelength λ, n_r is the refractive index of the medium (n_r = 1.4), Q_D is the donor quantum yield, κ^2 is an orientation factor. Assuming random reorientation of the donor emission and acceptor absorption transition moments during the emission lifetime (κ^2 = 0.67) R_o value was estimated to be 3.5 nm for ABM–SQ-1 and 6.4 nm for SQ-1–V2 donor–acceptor pairs.

3. Results and discussion

ABM is featured by several photophysical properties which make this probe especially attractive for biomolecular studies. These include: (i) large Stokes shift; (ii) high extinction coefficient; (iii) very weak fluorescence in an aqueous phase; (iv) high sensitivity of fluorescence parameters to environmental polarity [30]. Intramolecular charge transfer from the amine substituent to carbonyl group leads to substantial increase of ABM dipole moment after excitation. This, in turn, gives rise to reorientation of solvent dipoles around the probe excited-state dipole (solvent relaxation) and energy loss which manifests itself in a red shift of emission maximum (λ_{em}). Specifically, λ_{em} value of ABM exhibits shift from 583 nm in non-polar solvent benzene to 650 nm in polar solvent ethanol [30]. As illustrated in Fig. 1, addition of fibrillar lysozyme to ABM in buffer resulted in considerable increase of fluorescence intensity with λ_{em} around 580 nm being suggestive of the dye transfer into non-polar environment. To interpret this effect quantitatively, the observed dependency of fluorescence increase at 580 nm ($\Delta I_{580}(P)$) on protein concentration (Fig. 2A) was analyzed in terms of the Langmuir adsorption model (Eq. (2)), thereby yielding association constant and the number of binding sites. For the

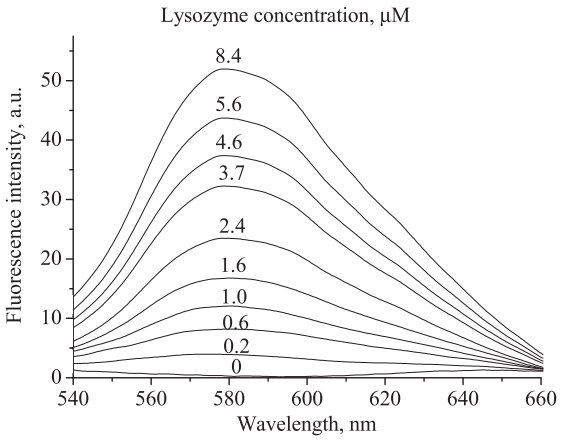

Fig. 1. Emission spectra of ABM recorded at varying concentrations of fibrillar lysozyme. ABM concentration was 0.5 μM.

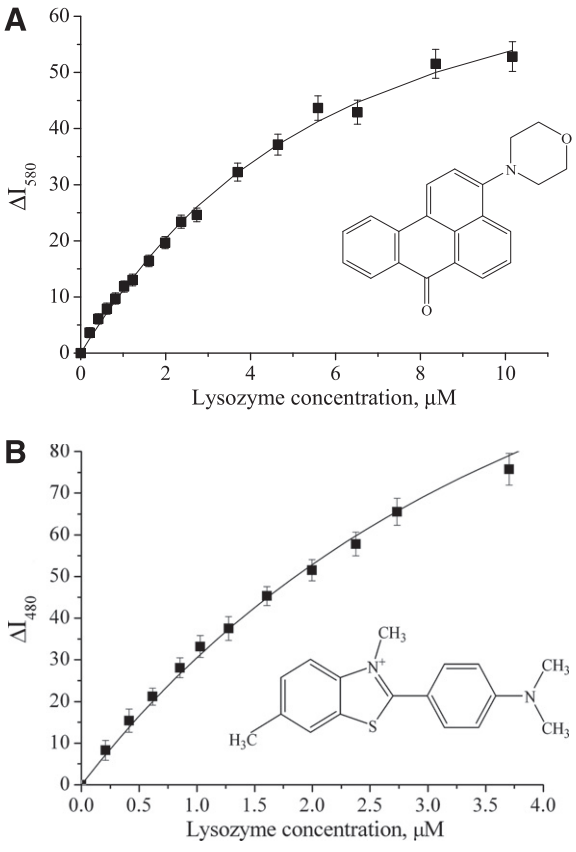

Fig. 2. The isotherms of ABM (A) and Thioflavin T (B) binding to lysozyme fibrils. Dye concentration was 0.5 μM (ABM) or 7.9 μM (ThT). Shown in insets are structural formulas of ABM (A) and ThT (B).

sake of comparison, analogous parameters were derived from $\Delta I_{480}(P)$ plots for classical amyloid marker ThT (Fig. 2B). As seen in Table 1, ABM affinity for fibrillar lysozyme turned out to be two orders of magnitude higher than that of ThT. Moreover, ABM molar fluorescence (the quantity proportional to the dye quantum yield in a fibrillar environment) exceeds analogous parameter of ThT by a factor of *ca.* 7.5. Additional advantage of ABM is associated with the large Stokes shift (*ca.* 140 nm) which leads to insignificant contribution of the scattered excitation light to emission spectra. On the contrary, in ThT assay care should be taken for possible distortion of fluorescence spectra by the light scattering. Last, ABM binding to native lysozyme appeared to be much weaker compared to fibrillar protein. For instance, at protein concentration 8 μM ABM fluorescence intensity increased by a factor of *ca.* 1.3 in the presence of native lysozyme, while fibrillar protein brought about 49-fold fluorescence increase. Taken together, all above findings strongly suggest that ABM displays more pronounced amyloid-sensing abilities than ThT. The cavities, channels or grooves, abundant in the structure of amyloid fibrils, can serve as potential binding sites for ABM. Molecular dimensions of ABM (long axis *ca.* 1.3 nm, short axis *ca.* 0.7 nm) are close to ThT size (long axis *ca.* 1.5 nm, short axis *ca.* 0.6 nm). It cannot be excluded that fibril location of ABM is similar to that of ThT, which is assumed to reside in a cavity with a diameter of 0.8–0.9 nm with the dye long axis being parallel to the long axis of the fibril [8,9].

To gain deeper insight into the properties of ABM environment in lysozyme fibrillar structures, we conducted a series of experiments addressing a solvent relaxation phenomenon. In steady-state fluorescence measurements this phenomenon manifests itself in the red shift of emission maximum with increasing excitation wavelength [31]. As illustrated in Fig. 3, emission maximum of fibril-bound ABM exhibits gradual red shift as excitation wavelength increases from 390 to 460 nm. Red-edge excitation shift has been observed for a variety of solvent sensitive dyes in a polar environment [29]. This effect is interpreted as arising from incomplete relaxation of solvent dipoles in fluorophore surrounding during fluorescence lifetime. The occurence of REES in the systems under study suggest that in lysozyme fibrillar aggregates ABM occupies polar sites where mobility of hydrated molecular groups in the vicinity of the fluorophore is substantially restricted compared to the bulk.

Table 1
Quantitative parameters of the dye binding to fibrillar lysozyme.

Dye	K_a (μM^{-1})	n (mol/mol)	a (μM^{-1})
ABM	1.2 ± 0.3	0.2 ± 0.06	165 ± 38
ThT	0.04 ± 0.01	7.6 ± 2.1	22 ± 5
SQ1	4.4 ± 1.1	0.25 ± 0.08	4.5 ± 1.4
V2	1.8 ± 0.5	0.6 ± 0.17	4.7 ± 1.3

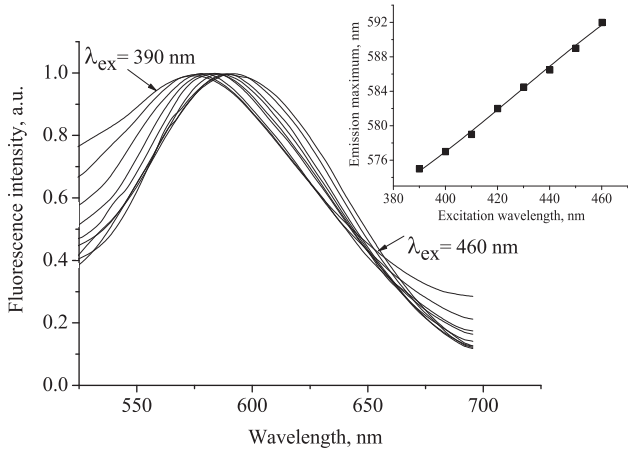

Fig. 3. Fluorescence spectra of fibril-bound ABM recorded at varying excitation wavelength. The inset shows the red shift of emission maximum with increasing excitation wavelength. Concentration of fibrillar lysozyme was 2 μM, ABM concentration was 4.8 μM.

At the next step of the study we employed resonance energy transfer technique to uncover the structural peculiarities of lysozyme fibrils. ABM, squaraine dye SQ-1 and polymethine dye V2 serve as the components of two donor–acceptor pairs, ABM–SQ-1 and SQ-1–V2. The results of RET measurements have been analyzed in terms of the stretched exponential model [32]:

$$Q_r = \int_0^\infty \exp\left(-\lambda - C_A V_d \Gamma(1 - d/6)\lambda^{\frac{d}{6}}\right) d\lambda \quad (3)$$

where $\lambda = t/\tau_D$, τ_D is the donor fluorescence lifetime in the absence of acceptor; $V_d = \pi^{\frac{d}{2}} R_o^d / \Gamma(\frac{d}{2}+1)$ is the volume of d-dimensional sphere of radius R_o, d is the dimensionality of fluorophore distribution (fractal-like dimension); $C_A = C_B/C_P V_{PF}$, C_P is the total protein concentration; V_{PF} is the volume of lysozyme molecule in a fibrillar state, C_B is the molar concentration of bound acceptor which was calculated from Eq. (1) using the binding parameters presented in Table 1. First, we approximated the observed RET profiles (Fig. 4) by Eq. (3) taking the R_o values valid for the isotropic and dynamic averaging conditions, when donors and acceptors are rapidly tumbling and their transition dipoles can adopt all orientations in a time short compared with the transfer time. Shown in Fig. 5A are the sets of model parameters $\{V_{PF}, d\}$ providing the best fit of the experimental data for $\kappa^2 = 0.67$. Evidently, if the above assumption about random fluorophore orientation was valid, the $V_{PF}(d)$ dependencies

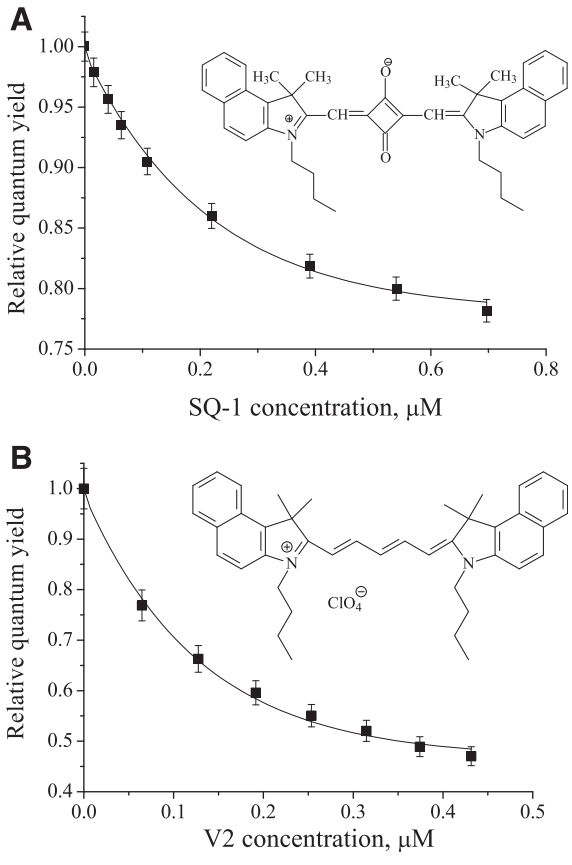

Fig. 4. Relative quantum yield of ABM (A) and SQ-1 (B) as a function of acceptor concentration. Concentration of fibrillar lysozyme was 10.2 μM (A) or 15.9 μM (B). Shown in insets are structural formulas of SQ-1 (A) and V2 (B).

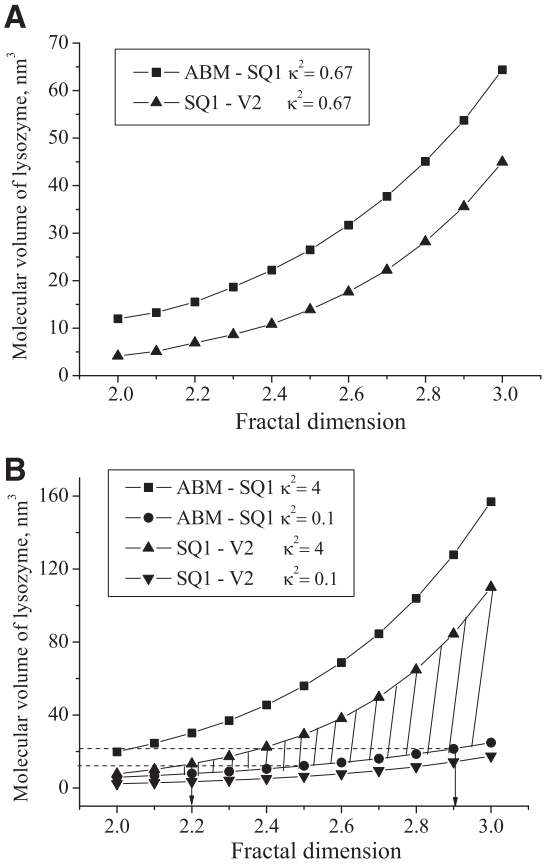

Fig. 5. Relationships between molecular volume of fibrillar lysozyme and its fractal dimension derived from the approximation of RET profiles (Fig. 4) by Eq. (3) taking isotropic value of orientation factor (0.67) (A) and varying κ^2 within the limits 0.1–4 (B).

recovered for the two donor–acceptor pairs would intersect each other at a certain point (V^*_{PF}, d^*) characterizing the volume per protein molecule and dimensionality of lysozyme fibrils. The absence of such an intersection implies that in our case the isotropic value of orientation factor (0.67) is inappropriate for R_o calculation. In keeping with this idea, the observed high values of fluorescence anisotropy (0.33 for ABM, 0.31 for SQ-1 and 0.18 for V2) indicate that rotational mobility of donors and acceptors is substantially restricted in a fibrillar environment. To circumvent the problem of unknown orientation factor, in the subsequent analysis of RET data κ^2 was allowed to vary within the widest possible limits corresponding to perpendicular ($\kappa^2 = 0$) and parallel donor and acceptor dipoles ($\kappa^2 = 4$) [29]. The overlap between the regions bounded by the limiting $V_{PF}(d)$ curves obtained for ABM–SQ-1 and SQ-1–V2 donor–acceptor pairs delineates an area of the most probable $\{V_{PF}, d\}$ sets (hatched area in Fig. 4B). This area can further be narrowed by defining the range of meaningful V_{PF} values. The partial specific volume (v^o) of lysozyme in its native state is *ca.* 0.71 ml/g, the value corresponding to molecular volume *ca.* 16.9 nm^3 per protein monomer [33]. Available data on volumetric properties of amyloid fibrils suggest that the sign and magnitude of the volume change upon fibrillization depend on the protein type and ambient conditions. Specifically, β_2-microglobulin [34], transthyretin and α-synuclein [35] exhibited volume increase, while poly-D-lysine, insulin and K3 peptide showed the opposite trend [34,36]. These differences in volumetric behavior reflect a subtle balance between v^o determinants, including van der Waals and excluded volumes, cavity volume, hydration and thermal terms [34]. Remarkably, the magnitude of volume changes on the protein transition from native to fibrillar state falls in the range ±30%. For instance, in the case of disulfide-deficient variant of hen lysozyme v^o value was found to increase from 0.68 to 0.72 ml/g upon monomer transformation into protofibrils [37]. Based on these experimental facts we concluded that meaningful limits for molecular volume of lysozyme in a fibrillar state are ~12–22 nm^3. Setting of these limits (dashed lines in Fig. 5B) gave the lower (2.2) and upper (2.9) bounds for fractal-like dimension d. It should be noted that $V_{PF}(d)$ plots obtained for $\kappa^2 < 0.1$ were not considered here because they lie beyond the range of reasonable V_{PF} values. Importantly, the suggested procedure of narrowing the range of model parameters can be more effective while employing several donor–acceptor pairs differing in the critical distance of energy transfer.

In this context it seems of significance to emphasize that RET technique per se does not permit determination of real fractal dimension, because energy transfer is measured on the length scale not exceeding two Forster radii. For this reason, here we refer to fractal-like dimension [38], whose values less than 3 are indicative of the system heterogeneity, not true fractality.

Fractal dimension depends on the scaling between mass and size of polypeptide chain, being a measure of protein compactness. This parameter has been estimated for native (d ~2.2–2.8 [39]), denaturated (d ~2.5–1.8 [40,41]) and aggregated (d ~2.7 [42]) proteins. Loosening of the protein structure under denaturing conditions is followed by the reduction of fractal dimension, as was demonstrated, particularly, for bovine serum albumin (d decreases from 2.3 to 1.8 [41]) and lysozyme (d decreases from 2.8 to 2.5 [40]).

To summarize, the present study revealed an important new feature of the fluorescent benzanthrone dye ABM, *viz.* its amyloid specificity. Compared to classical amyloid marker ThT, this dye displays: (i) greater extent of fluorescence increase, (ii) higher affinity for fibrillar structures, (iii) weaker binding to the native protein, (iv) larger Stokes shift. Resonance energy transfer measurements involving ABM, squaraine dye SQ-1 and polymethine dye V2 demonstrated principal possibility of clarifying the structural peculiarities of fibrillar aggregates through analyzing the RET data from several donor–acceptor pairs.

Acknowledgements

This work was supported by the grants from European Social Fund (project number 2009/0205/1DP/1.1.1.2.0/09/APIA/VIAA/152), the Science and Technology Center in Ukraine (project number 4534) and Fundamental Research State Fund (project number F.28.4/007). V.T. gratefully acknowledges an award by Human Frontier Science Program. The authors are indebted to referees for valuable remarks.

References

[1] A.M. Morris, M.A. Watzky, R.G. Finke, Biochim. Biophys. Acta 1794 (2009) 375.
[2] M. Stefani, Biochim. Biophys. Acta 1739 (2004) 5.
[3] S. Idicula-Thomas, P.V. Balaji, Curr. Sci. 92 (2007) 758.
[4] L.C. Serpell, Biochim. Biophys. Acta 1502 (2000) 16.
[5] R. Khurana et al., Biophys. J. 85 (2003) 1135.
[6] M.R. Nilsson, Methods 34 (2004) 151.
[7] L.A. Munishkina, A.L. Fink, Biochim. Biophys. Acta 1768 (2007) 1862.
[8] M.R.H. Krebs, E.H.C. Bromley, A.M. Donald, J. Struct. Biol. 149 (2005) 30.
[9] M. Groenning, J. Chem. Biol. 3 (2010) 1.
[10] H. LeVine III, Protein Sci. 2 (1993) 404.
[11] K. Murakami et al., J. Biol. Chem. 278 (2003) 46179.
[12] M. Lindgren, K. Sorgjerd, P. Hammarstrom, Biophys. J. 88 (2005) 4200.
[13] H. LeVine III, Arch. Biochem. Biophys. 342 (1997).
[14] M. Mauro, E.F. Craparo, A. Podesta, et al., J. Mol. Biol. 366 (2007) 258.
[15] S.A. Hudson, H. Ecroyd, T.W. Kee, J.A. Carver, FEBS J. 276 (2009) 5960.
[16] H. Kowa et al., Am. J. Pathol. 165 (2004) 273.
[17] A.S. Crystal, B.I. Giasson, A. Crowe, M.-P. Kung, Z.S.-P. Zhuang, J.Q. Trojanowski, V.M. Lee, J. Neurochem. 86 (2003) 1359.

[18] S.D. Styren, R.L. Hamilton, G.C. Styren, W.E. Klunk, J. Histochem. Cytochem. 48 (2000) 1223.
[19] J.S. Ahn, J.H. Lee, J.H. Kim, S.R. Paik, Anal. Biochem. 367 (2007) 259.
[20] J. Kardos et al., Biochim. Biophys. Acta 1753 (2005) 108.
[21] K.D. Volkova, V.B. Kovalska, A.O. Balanda, R.J. Vermeij, V. Subramaniam, Yu.L. Slominskii, S.M. Yarmoluk, J. Biochem. Biophys. Methods 70 (2007) 727.
[22] C.J. Sigurdson et al., Proc. Natl. Acad. Sci. USA 106 (2009) 304.
[23] I. Kalnina et al., Proc. Latv. Acad. Sci. 60 (2006) 113.
[24] I. Kalnina, L. Klimkane, E. Kirilova, M.M. Toma, G. Kizane, I. Meirovics, J. Fluoresc. 17 (2007) 619.
[25] E.M. Kirilova, I. Kalnina, Appl. Biochem. Biotechnol. 160 (2010) 1744.
[26] E.M. Kirilova, I. Meirovics, S.V. Belyakov, Chem. Heterocycl. Comp. 7 (2002) 896.
[27] V.M. Ioffe, G.P. Gorbenko, T. Deligeorgiev, N. Gadjev, A. Vasilev, Biophys. Chem. 128 (2007) 75.
[28] M. Holley, C. Eginton, D. Schaefer, L.R. Brown, Biochem. Biophys. Res. Commun. 373 (2008) 164.
[29] J.R. Lakowicz, Principles of Fluorescent Spectroscopy, third edn., Springer, New York, 2006.
[30] E.M. Kirilova, I. Kalnina, G.K. Kirilov, I. Meirovics, J. Fluoresc. 18 (2008) 645.
[31] R. Hutterer, F.W. Schneider, H. Sprinz, M. Hof, Biophys. Chem. 61 (1996) 151.
[32] J.M. Drake, J. Klafter, P. Levitz, Science 251 (1991) 1574.
[33] K. Gekko, H. Noguchi, J. Phys. Chem. 83 (1979) 2706.
[34] Y.-H. Lee, E. Chatani, K. Sasahara, H. Naiki, Y. Goto, J. Biol. Chem. 284 (2009) 2169.
[35] D. Foguel et al., Proc. Natl. Acad. Sci. USA 100 (2003) 9831.
[36] V. Smirnovas, R. Winter, T. Funck, W. Dzwolak, Chem. Phys. Chem. 7 (2006) 1046.
[37] K. Akasaka, A.R.A. Latif, A. Nakamura, K. Matsuo, H. Tachibana, K. Gekko, Biochemistry 46 (2007) 10444.
[38] J. Schleicher, M. Hof, F.W. Schneider, Ber. Bunsenges. Phys. Chem. 97 (1993) 172.
[39] M.B. Enright, D.M. Leitner, Phys. Rev. E 71 (2005) 011912.
[40] S.G. Lushnikov, A.V. Svanidze, S.N. Gvasaliya, G. Torok, L. Rosta, I.L. Sashin, Phys. Rev. E 79 (2009) 031913.
[41] S.H. Chen, J. Teixeira, Phys. Rev. Lett. 57 (1986) 2583.
[42] A. Podesta, G. Tiana, P. Milani, M. Manno, Biophys. J. 90 (2006) 589.